biology letters

How interactions between animal movement and landscape processes modify local range dynamics and extinction risk

Damien A. Fordham, Kevin T. Shoemaker, Nathan H. Schumaker, H. Resit Akçakaya, Nathan Clisby and Barry W. Brook

Biol. Lett. 2014 **10**, 20140198, published 7 May 2014

biology letters

rsbl.royalsocietypublishing.org

Research

Cite this article: Fordham DA, Shoemaker KT, Schumaker NH, Akçakaya HR, Clisby N, Brook BW. 2014 How interactions between animal movement and landscape processes modify local range dynamics and extinction risk. *Biol. Lett.* **10**: 20140198.
http://dx.doi.org/10.1098/rsbl.2014.0198

Received: 4 March 2014
Accepted: 15 April 2014

Subject Areas:
ecology

Keywords:
dispersal, metapopulation, global change, individual-based model, population viability analysis, species distribution

Author for correspondence:
Damien A. Fordham
e-mail: damien.fordham@adelaide.edu.au

†These authors contributed equally to this study.

Electronic supplementary material is available at http://dx.doi.org/10.1098/rsbl.2014.0198 or via http://rsbl.royalsocietypublishing.org.

Royal Society Publishing

Global change biology

How interactions between animal movement and landscape processes modify local range dynamics and extinction risk

Damien A. Fordham[1,†], Kevin T. Shoemaker[2,†], Nathan H. Schumaker[3], H. Reşit Akçakaya[2], Nathan Clisby[1] and Barry W. Brook[1]

[1]The Environment Institute and School of Earth and Environmental Sciences, University of Adelaide, Adelaide, South Australia 5005, Australia
[2]Department of Ecology and Evolution, Stony Brook University, Stony Brook, NY 11794, USA
[3]US Environmental Protection Agency, 200 SW 35th St., Corvallis, OR 97333, USA

Forecasts of range dynamics now incorporate many of the mechanisms and interactions that drive species distributions. However, connectivity continues to be simulated using overly simple distance-based dispersal models with little consideration of how the individual behaviour of dispersing organisms interacts with landscape structure (functional connectivity). Here, we link an individual-based model to a niche-population model to test the implications of this omission. We apply this novel approach to a turtle species inhabiting wetlands which are patchily distributed across a tropical savannah, and whose persistence is threatened by two important synergistic drivers of global change: predation by invasive species and over-exploitation. We show that projections of local range dynamics in this study system change substantially when functional connectivity is modelled explicitly. Accounting for functional connectivity in model simulations causes the estimate of extinction risk to increase, and predictions of range contraction to slow. We conclude that models of range dynamics that simulate functional connectivity can reduce an important source of bias in predictions of shifts in species distributions and abundances, especially for organisms whose dispersal behaviours are strongly affected by landscape structure.

1. Introduction

Spatially explicit demographic models are increasingly being used to forecast the influence of global change on species' range dynamics in terrestrial [1] and marine [2] systems. This is because such models provide direct predictions of spatio-temporal patterns of abundance, allowing extinction risk to be estimated and conservation management efforts evaluated and prioritized [3]. The drawbacks are that these models are data intensive and require a robust understanding of the population dynamics of the focal species for effective parameterization [4].

When embedded in demographic frameworks, models of species' range dynamics typically make use of simplifying assumptions to minimize the complexity of interactions between biotic and landscape processes. Such simplifications increase uncertainty and can result in unwanted bias in forecasts of extinction risk and range shifts, potentially affecting conservation actions [5]. Methods used to estimate and model connectivity have been singled out as particularly important sources of uncertainty in climate-driven predictions of species ranges and abundances [6]. Improving techniques for simulating dispersal in models of range dynamics should therefore be viewed as a research

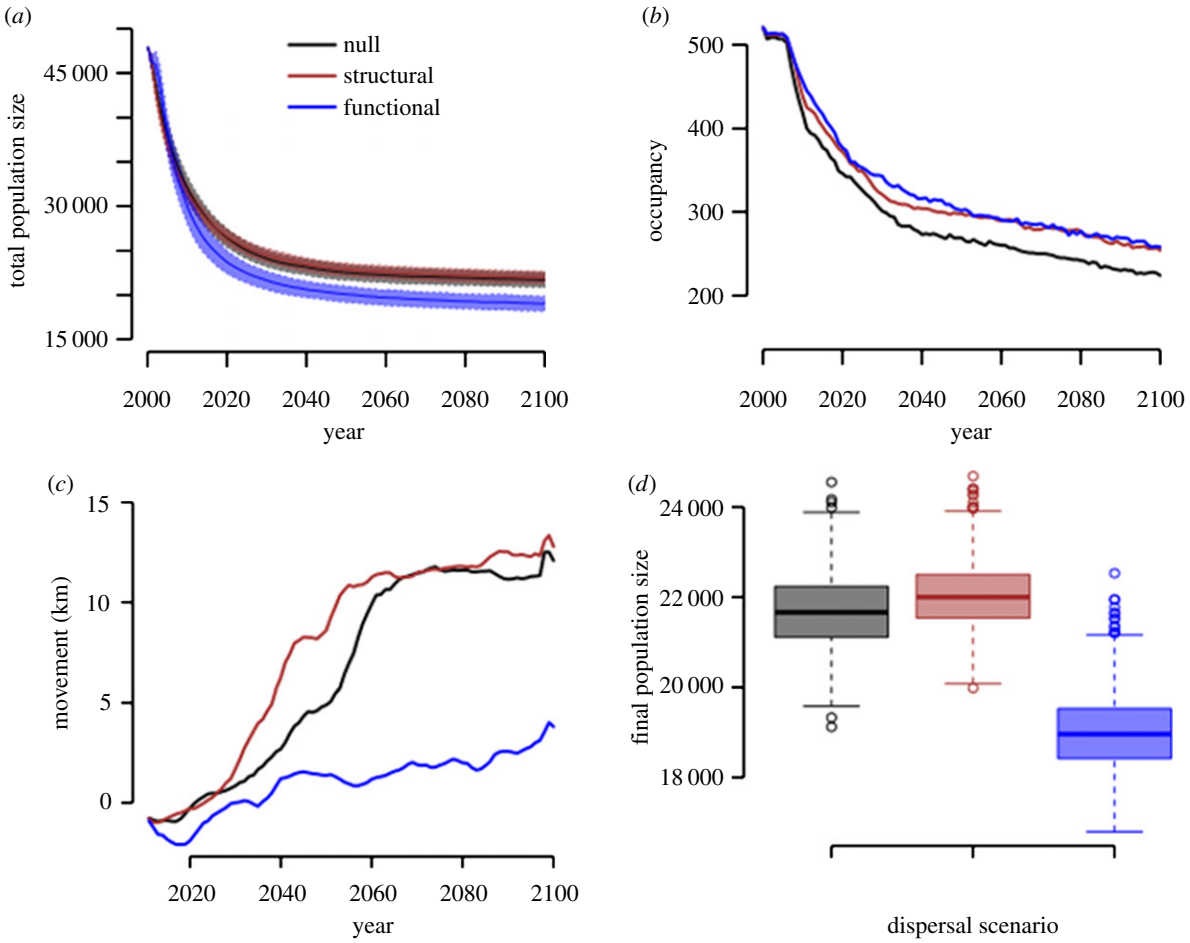

Figure 1. The influence of structural and functional connectivity on predicted range dynamics and extinction risk. Shown are mean population estimates (solid line), including fifth and 95th percentiles of population size (*a*), average number of extant populations (*b*), movement of the southern range boundary in a northerly direction (*c*) and final population size (*d*) derived from a stochastic metapopulation model for the freshwater turtle *Chelodina rugosa* according to three connectivity scenarios: null (black), structural (red) and functional (blue). Note that there is strong agreement in forecast population size according to the null and structural dispersal scenarios.

priority, especially because enhancing connectivity is the most commonly proposed solution for conserving biodiversity under climate change [7].

In demographic models of species' range dynamics, the dispersal process is usually approximated using a simple distance-based dispersal kernel, which is often extrapolated from field-based estimates of average and maximum path lengths observed within a single or limited number of populations [8]. Actual dispersal patterns depend on structural and functional connectivity. Structural connectivity refers to the effects of population-level dispersal conduits or barriers, whereas functional connectivity refers to interactions between the behaviour of dispersing individuals and structural elements of the landscape and environmental processes [9]. For example, streams may serve as dispersal conduits for a species (structural connectivity), and long-distance dispersal may occur primarily via sporadic flood events that carry young individuals searching for territories in a downstream direction (functional connectivity). Structural connectivity has been integrated into forecasts of range dynamics using spatially explicit demographic models [10], mainly via least-cost pathway approaches that identify the optimal route between two patches on the basis of a gridded cost surface representing the resistance of the intervening matrix [11]. By contrast, functional connectivity is rarely considered in forecasts of species' range dynamics (but see [12]) and has not been considered in detail in spatially explicit demographic models. This is despite the development of mechanistic individual- or agent-based models capable of assigning behaviour to individuals and allowing them to interact directly with their surroundings [13].

Niche-population models couple ecological niche models with stochastic demographic models and have recently been used to link multiple mechanisms and interactions that together drive species distributions and abundances [3]. In this study, we determine the sensitivity of niche-population model forecasts of range dynamics and extinction risk to characterizations of landscape connectivity as strictly structural, or as truly functional—incorporating both landscape structure and animal-movement behaviour. To account for functional connectivity, we link niche-population models to spatially explicit individual-based models. We then apply this novel approach to a well-studied freshwater turtle species from northern Australia (*Chelodina rugosa*), which is threatened by synergistic drivers of global change (predation by invasive species, habitat degradation and overexploitation) in a tropical wetland environment [14].

2. Material and methods

We constructed spatially explicit stage- and sex-based stochastic matrix models for *C. rugosa* in two neighbouring water catchments in northern Australia using the RAMAS GIS v. 5

software [15]. The region is bounded by distinct northern (saltwater) and southern (sandstone escarpment) local range boundaries. We modelled the influence of invasive species and overexploitation (and their interaction) [14] on local population dynamics at 521 waterholes, patchily distributed within a terrestrial habitat. We used repeat survey data from 50 waterholes (1999–2007) and linear regression to determine waterhole ephemerality (frequency of drying and hydroperiod). The surveyed waterholes captured the environmental features of the study region, meaning that the statistical model was not used to extrapolate to novel environmental conditions. The ephemerality of waterholes varied spatio-temporally (based on observed local rainfall between 1980 and 2005), affecting rates of turtle predation by pigs and humans and their interaction [16], and resulting in some refuge populations with low predation rates. We did not consider an effect of future global warming on ephemerality.

We modelled dispersal between distinct habitat patches using: (i) a simple distance-based dispersal kernel extrapolated from field-based estimates of average and maximum *C. rugosa* movement (*null model*); (ii) a least-cost pathway method that combined a friction map with a distance-based dispersal kernel [15], thus allowing dispersal patterns to be affected by habitat characteristics such as dispersal barriers as well as inter-patch distance (*structural connectivity model*); and (iii) a spatially explicit individual-based model that incorporated mechanisms linking complex turtle movement behaviour to habitat structure (*functional connectivity model*). The influence of dispersal on spatial abundance patterns and local range limits was simulated using 10 000 stochastic replicates, run over a 101 year period (i.e. 2000–2100) with a 10 year initial burn-in (stabilization) period. Population viability was assessed using expected minimum abundance (EMA) calculated for the period 2010–2100. Range movement between 2010 and 2100 was calculated annually based on the latitude of the geographical centre of the most southern subpopulation [17]. Change in the number of occupied waterholes and total population abundance (of persistent model runs) over time were also investigated. See the electronic supplementary material, appendices S1 and S2 for additional technical details.

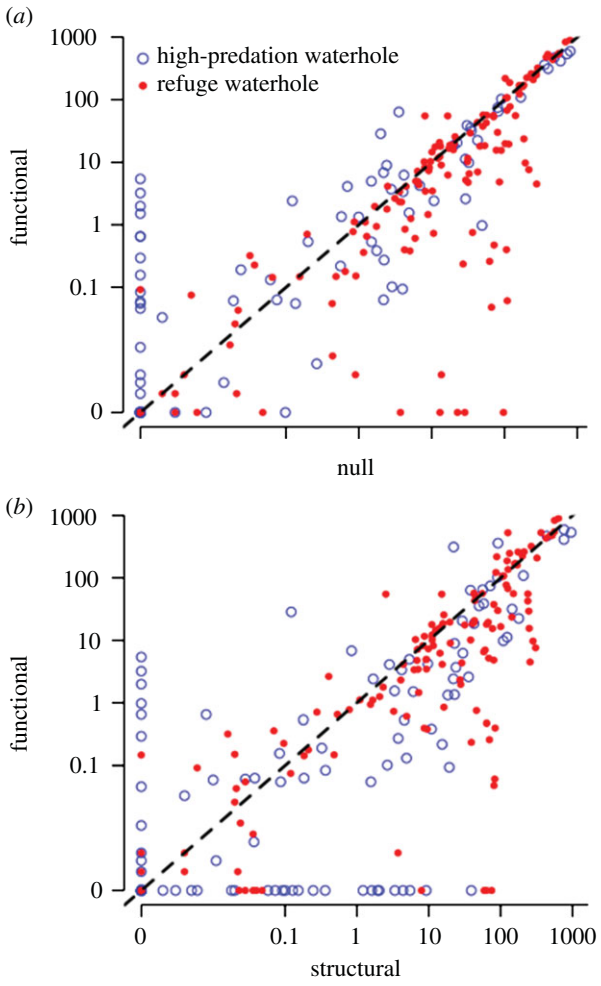

Figure 2. The influence of functional connectivity on local expected minimum abundance ($\log_{10}$ scale) in populations subject to high (high-predation waterhole) and low (refuge waterhole) levels of predation. Plots compare results from simulations with functional connectivity to those without (top) and with (bottom) structural connectivity.

3. Results

Accounting for functional connectivity caused turtle population abundance to decline at a faster rate compared with models that did not link movement behaviour to landscape structure explicitly (figure 1). Populations with high predation pressure tended to persist for longer (83 versus 62 pig-predated populations remained extant in 2100), and refuge populations (no pig predation) tended to have lower EMA (49 versus 59) under the functional connectivity scenario compared with the null scenario (table 1, percentage decline in high predation populations; figure 2*a*). The median size of refuge populations in 2100 was smaller for the functional connectivity scenario (28) compared with the structural (77) and null scenarios (55) (electronic supplementary material, figure S1). Although the predicted number of extant populations in 2100 was similar under the functional and structural connectivity scenarios (table 1), the populations that were predicted to experience extirpation differed between these scenarios (figure 2). The southern range boundary contracted in a northerly direction at a much slower rate under the functional connectivity scenario (figure 1), moving 3.81 km by 2100, compared with more than 12 km for the null and structural connectivity scenarios (table 1). Turtle populations with high predation rates tended to persist for shorter periods in savannah versus floodplain environments (electronic supplementary material, figure S2).

4. Discussion

By coupling individual-based and niche-population models, we show that estimates of extinction risk and local range movement are sensitive to alternative characterizations of landscape connectivity. Accounting for the interaction between animal behaviour and landscape structure (functional connectivity) in model simulations for *C. rugosa* results in elevated local population-level extinction risk and slower rates of local range contraction. Projected shifts in turtle abundance and range margins derived from the null (distance-based dispersal) and structural connectivity models (dispersal affected by land cover characteristics as well as inter-patch distance) were more similar to each other than to results obtained from the functional connectivity model. These results suggest that: (i) functional connectivity should be considered in models of species' range dynamics when the behaviour of the dispersing organism is affected by landscape structural elements and processes; and (ii) high rates of extirpation of populations along a trailing range boundary can occur without causing extensive range movement, despite resulting in substantial declines in population abundance and occupancy.

The influence of landscape connectivity on plant and animal movement is a vital component of metapopulation ecology,

Table 1. Range movement and extinction risk according to three contrasting methods of modelling connectivity. Expected minimum abundance as a proportion of initial population size (EMA), number of subpopulations in the metapopulation (metapop size), movement of the southern range boundary in a northerly direction, and percentage of high-predation (predation) and low predation (refuge) populations remaining in savannah and floodplain habitats in 2050 and 2100 according to three connectivity scenarios: null, structural and functional (see Material and methods for details).

year	connectivity scenario	EMA	metapop size	movement (km)	high-predation savannah (%)	high-predation floodplain (%)	refuge savannah (%)	refuge floodplain (%)
2050	null	0.46	269	4.89	15	28	74	68
	structural	0.47	298	8.6	22	41	76	68
	functional	0.41	302	1.38	20	33	70	63
2100	null	0.43	224	12.09	14	25	54	63
	structural	0.44	254	12.79	20	32	66	58
	functional	0.43	258	3.8	20	30	67	57

influencing fundamental processes such as population dynamics and evolution [18]. However, the simplifying assumptions commonly used for modelling connectivity in metapopulation models and ecological network analysis are likely to bias forecasts of population persistence [19] and range movement. During the wet season, *C. rugosa* move to the shallows to feed at the expanding margins of waterholes. This feeding behaviour results in increased contact with streams, allowing turtles to more easily disperse to geographically distant and isolated waterholes. Simulations that included this behaviour resulted in slower rates of range contraction owing to pig predation and an increased mean frequency of dispersal into populations experiencing high predation rates (demographic sinks), resulting in lower densities in refuge populations (demographic sources). This suggests a more general result—that failing to consider important functional connectivity in models of range dynamics is likely to underestimate extinction risk and overestimate range shifts for species such as *C. rugosa* that interact with landscape features such as dispersal corridors (natural or artificial).

Our spatio-temporally complex wetland system is well suited for examining the importance of functional and structural connectivity. The preferred habitat of *C. rugosa*—ephemeral wetlands that occasionally or regularly dry—provides a gradient in resource quality that varies through both space and time. While our results suggest that many demographic-based forecasts of range movement and extinction risk will be improved by including functional connectivity, it is likely that biases in model forecasts for some species can be addressed adequately without the need for behaviourally explicit individual-based models. For example, previous niche-population model predictions for marine species with free-swimming larval stages [5] almost certainly would be improved by simulating dispersal as a passive process driven principally by oceanic currents.

Using spatially explicit demographic models with functional connectivity, we have confirmed that present-day estimates of turtle predation by pigs [14,16] are so high that the extirpation of many *C. rugosa* populations is very likely in the near term, particularly in waterholes embedded within savannah landscapes. Our results for floodplain turtle populations are likely to underestimate extinction risk, because we did not account for future sea-level rise, which is likely to result in severe regional habitat loss [20], further threatening the persistence of *C. rugosa*.

Funding statement. Australian Research Council supported D.A.F., B.W.B. and N.C. (DP1096427, FT100100200 and FS110200051). National Science Foundation supported K.T.S. and H.R.A. (DEB-1146198). The U.S. Environmental Protection Agency (EPA) supported N.H.S. and approved this paper for publication. Approval does not imply the content reflects the views of EPA.

References

1. Dullinger S *et al*. 2012 Extinction debt of high-mountain plants under twenty-first-century climate change. *Nat. Clim. Change* **2**, 619–622. (doi:10.1038/nclimate1514)
2. Cheung WWL, Sarmiento JL, Dunne J, Frolicher TL, Lam VWY, Deng Palomares ML, Watson R, Pauly D. 2012 Shrinking of fishes exacerbates impacts of global ocean changes on marine ecosystems. *Nat. Clim. Change* **3**, 254–258. (doi:10.1038/nclimate1691)
3. Fordham DA, Akcakaya HR, Araujo MB, Keith DA, Brook BW. 2013 Tools for integrating range change, extinction risk and climate change information into conservation management. *Ecography* **36**, 956–964. (doi:10.1111/j.1600-0587.2013.00147.x)
4. Schurr FM *et al*. 2012 How to understand species' niches and range dynamics: a demographic research agenda for biogeography. *J. Biogeogr.* **39**, 2146–2162. (doi:10.1111/j.1365-2699.2012.02737.x)
5. Fordham DA *et al*. 2013 Population dynamics can be more important than physiological limits for determining range shifts under climate change. *Glob. Change Biol.* **19**, 3224–3237. (doi:10.1111/gcb.12289)
6. Travis JMJ *et al*. 2013 Dispersal and species' responses to climate change. *Oikos* **122**, 1532–1540. (doi:10.1111/j.1600-0706.2013.00399.x)
7. Heller NE, Zavaleta ES. 2009 Biodiversity management in the face of climate change: a review of 22 years of recommendations. *Biol. Conserv.* **142**, 14–32. (doi:10.1016/j.biocon.2008.10.006)
8. Hein S, Pfenning B, Hovestadt T, Poethke HJ. 2004 Patch density, movement pattern, and realised dispersal distances in a patch-matrix landscape: a simulation study. *Ecol. Model.* **174**, 411–420. (doi:10.1016/j.ecolmodel.2003.10.005)
9. Baguette M, Dyck H. 2007 Landscape connectivity and animal behavior: functional grain as a key determinant for dispersal. *Landsc. Ecol.* **22**, 1117–1129. (doi:10.1007/s10980-007-9108-4)
10. Fordham DA, Akçakaya HR, Brook BW, Rodríguez A, Alves PC, Civantos E, Triviño MJ, Watts MJ, Araújo MB. 2013 Adapted conservation measures are required to save the Iberian lynx in a changing

climate. *Nat. Clim. Change* **3**, 899–903. (doi:10.1038/nclimate1954)

11. Urban DL, Minor ES, Treml EA, Schick RS. 2009 Graph models of habitat mosaics. *Ecol. Lett.* **12**, 260–273. (doi:10.1111/j.1461-0248.2008.01271.x)
12. Zurell D, Grimm V, Rossmanith E, Zbinden N, Zimmermann NE, Schröder B. 2012 Uncertainty in predictions of range dynamics: black grouse climbing the Swiss Alps. *Ecography* **35**, 590–603. (doi:10.1111/j.1600-0587.2011.07200.x)
13. Grimm V, Railsback SF. 2005 *Individual-based modelling and ecology*. Princeton, NJ: Princeton University Press.
14. Fordham DA, Georges A, Brook BW. 2008 Indigenous harvest, exotic pig predation and local persistence of a long-lived vertebrate: managing a tropical freshwater turtle for sustainability and conservation. *J. Appl. Ecol.* **45**, 52–62. (doi:10.1111/j.1365-2664.2007.01414.x)
15. Akcakaya HR, Root WT. 2005 *RAMAS GIS: linking landscape data with population viability analysis* (*version 5.0*). Setaukey, NY: Applied Biomathematics.
16. Fordham DA, Georges A, Brook BW. 2007 Demographic response of snake-necked turtles correlates with indigenous harvest and feral pig predation in tropical northern Australia. *J. Anim. Ecol.* **76**, 1231–1243. (doi:10.1111/j.1365-2656.2007.01298.x)
17. Watts MJ, Fordham DA, Akçakaya HR, Aiello-Lammens ME, Brook BW. 2013 Tracking shifting range margins using geographical centroids of metapopulations weighted by population density. *Ecol. Model.* **269**, 61–69. (doi:10.1016/j.ecolmodel.2013.08.010)
18. Hanski I. 1999 *Metapopulation ecology*. Oxford, UK: Oxford University Press.
19. Fletcher RJ, Acevedo MA, Reichert BE, Pias KE, Kitchens WM. 2011 Social network models predict movement and connectivity in ecological landscapes. *Proc. Natl Acad. Sci. USA* **108**, 19 282–19 287. (doi:10.1073/pnas.1107549108)
20. Traill LW, Bradshaw CJA, Delean S, Brook BW. 2010 Wetland conservation and sustainable use under global change: a tropical Australian case study using magpie geese. *Ecography* **33**, 818–825. (doi:10.1111/j.1600-0587.2009.06205.x)

Appendix S1: Online Extended Methods

We used spatially explicit demographic models to simulate the metapopulation dynamics of *Chelodina rugosa* (northern snake-necked turtle) in two neighbouring water catchments in northern Australia: the Blythe and Liverpool river catchments. The region was chosen because the population dynamics of *C. rugosa* in these catchments is well established [1-7].

Survey data

We surveyed 80 waterholes repeatedly over an eight year period (1999-2007) to determine: drying frequency, duration of inundation, extent of pig rooting, vegetation composition and rates of turtle harvest carried out by the indigenous people. Turtle occurrence was assessed in the year 2000, between May and September, using hoop traps baited with fish [8]. We used 10-15 traps (exact number depended on the size of the waterhole) which we re-baited and moved once over a 4 night trapping period. Traps were evenly spread throughout the waterhole to depths of 1.2 metres. Drying frequency (DRYFREQ) was averaged across years and classed as either: drying frequently (≥ 20% of years, typically drying every other year: DRYFREQ = 0.5), rarely drying (< 20 % of years, typically drying every 6 years: DRYFREQ = 0.166) or no drying. Period of inundation (hydroperiod) was calculated by recording the month of drying in each year. The average waterhole hydroperiod was classed as either: (i) too short to support *C. rugosa* or *Eleocharis dulcis* (water chestnut plant) (EPHEM = 1: dries before August 1) or sufficient to support these species (EPHEM = 0: dries on or after August 1). The extent of pig rooting at the end of the dry season (late October/ early November) was assessed both visually, and using direct measures described by Fordham *et al.* [3]. Pig rooting intensity (PIGROOT) was classed as being high (PIGROOT = 1) if on average ≥ 20 % of the surface area of the waterhole was impacted by pig rooting in a given year; and low (PIGROOT = 0) if < 20 % of the area was impacted. The vegetation composition was surveyed and the area of the waterhole comprising *E. dulcis* was estimated and assigned one of two categories: high-to-medium (ELEOCHARIS = 1: ≥ 10 %), or low (ELEOCHARIS = 0: < 10%). An identical

area-based assessment was made for *Melaleuca sp.* Harvest frequency (HARVFREQ) was assessed using direct observations and surveys (see [7]).

Environmental spatial data

Wetland features were mapped using high resolution scans of 1:50,000 topographic maps produced by the Army Topographic Support Establishment (Department of Defence, Commonwealth of Australia) in 1999. Specifically, twenty four maps covering the Blyth and Liverpool catchments downstream of the Arnhem Land sandstone escarpment were scanned, geo-referenced and wetland features were digitised using ArcGIS 10. This produced a polygon map of waterhole features and their associated attributes: (i) VEG: vegetation density (1 = dense, 0 = sparse or absent); (ii) AREA: wetland area (ha); (iii) PERVEG: percent area of the waterhole that is vegetated; (iv) PERMANENT: whether the waterhole is inundated even during unusually dry years (1 = permanent, or 0 = ephemeral); and (v) SALTWATER: salinity content (1 = salt water, or 0 = fresh water). Wetland features were digitised at a 1:5,000 – 1:7,500 scale. A horizontal accuracy of 90% within ± 25m exists for features on the original topographic maps. We did not include the sandstone catchment area because *Chelodina burrungandjii*, not *C. rugosa*, is found in this region [9].

Digital spatial layers describing major road networks, water courses and towns and outstations (satellite communities) were accessed from GeoScience Australia (GEODATA TOPO 250K Series 3 - Online [via MapConnect]; ANZCW0703008969). The layers were used to calculate distances from each wetland feature to the nearest road (DISTROAD), river (DISTRIVER), and outstation (or town; DISTTOWN) using the *Near* function in Spatial Analyst ArcGIS v10. The National Vegetation Information System broadly describes the present-day vegetation of the Northern Territory of Australia [10] and was used to distinguish floodplain (SAVANNA = 0) and savannah (SAVANNA = 1) vegetation communities.

Elevation was based on a 30m Digital Terrain Model derived from the NASA SRTM project [11]. From this, slope was calculated using the 'DEM Surface Tools' ArcGIS extension [12]. A map

of plant available water capacity (PAWC, a measure of soil water available to plants at 250 x 250m grid-cell resolution) was accessed from the Australian Soil Resource Information System (http://www.asris.csiro.au). National soil data was provided by the Australian Collaborative Land Evaluation Program ACLEP (www.clw.csiro.au/aclep). All spatial layers are available from the authors on request.

Predictions of abundance and carrying capacity

Three features of waterholes were previously identified as key determinants of occurrence, abundance and vital rates for *C. rugosa*: the density of *E. dulcis* at a waterhole, the drying frequency, and the period of inundation [2, 3]. We used binary logistic regression to model the relationship between mapped environmental variables and: (i) ELEOCHARIS: presence of *E. dulcis* (observed density ≥ 10 % or < 10 %); and (ii) EPHEM: whether waterholes dry or not before August (a hydroperiod too short to support populations of *C. rugosa*). We used ordinary linear regression to model the relationship between mapped environmental variables and drying frequency (DRYFREQ; described above) (we compared logit-transformed and untransformed DRYFREQ models and found that modelling untransformed DRYFREQ as the response variable resulted in a slightly lower cross-validation error). Models were built using survey information from 50 ephemeral waterholes within the study region. We hypothesised *a priori* that these waterhole features are affected by elevation, slope, waterhole area (AREA), PAWC, being in a floodplain or savanna environment (SAVANNA), and vegetation density (VEG; see above for a description of spatial features). The final predictor set was selected by first eliminating highly correlated variables from the predictor set (one variable was retained for each pair with Pearson correlation > 0.75) and subsequently selecting the best-performing combination of predictor variables using stepwise AIC_c (Akaike Information Criterion, with a correction for limited sample size [13]). We calculated proportion of deviance explained (hereafter R^2 [14]) as a summary statistic to describe structural goodness-of-fit [15].

We assessed the predictive performance of the selected models using leave-one-out cross validation and subsequently computing area under the receiver operating curve (AUC) [16]. The best models for ephemerality (logit(EPHEM)= -0.17 - 9.4E-6*[AREA] + 0.18*[SAVANNA] – 18.7*[VEG], $R^2 = 0.35$) and drying frequency (DRYFREQ = 0.4 + 0.0028*PERVEG – 0.23*[SAVANNA]; $R^2 = 0.53$) exhibited adequate model performance (AUC > 0.8) [17]. However, cross validation for *E. dulcis* presence (i.e., ELEOCHARIS ≥ 10%) suggested poor predictive performance (AUC < 0.7). Therefore, we developed a simple set of rules based on field observations to predict *E. dulcis* presence in the Blythe and Liverpool catchments. We classified a waterhole as having *E. dulcis* if it dries regularly (> 20 % of years; DRYFREQ = 0.5) , but not before August [3] (EPHEM = 0); and if it is not a marine swamp, or if it is not a sparsely vegetated waterhole (VEG = 0) in a savanna habitat (SAVANNA = 1).

We used the spatial predictions of waterhole features (generated as described above) and area of the waterhole (number of 50m x 50m pixels) to predict the initial abundance and carrying capacity for each of the 1,013 waterholes in the study region. The surveyed waterholes captured the environmental features of the study region, meaning that modelled predictions of waterhole features did not extrapolate to novel environmental conditions. We used published [5] and unpublished capture-mark-recapture (CMR) estimates of abundance at waterholes differing in drying frequency and timing, density of *E. dulcis* and pig predation rates to calculate average abundance at waterholes. We set abundance as follows: (i) rarely drying waterholes (dries ≤ 20 % of years) with no *E. dulcis* = 5.5/ha; (ii) frequently drying waterholes (dries > 20 % of years) with *E. dulcis* = 9.5/ha; (iii) frequently drying waterholes with no *E. dulcis* = 5.5/ha; (iv) waterholes that dry annually before August = 0/ha; and (v) permanent waterholes = 3/ha. Predicted abundance was verified using an independent set of 10 waterholes with CMR estimates of average abundance. With the exception of one site, all model estimates agreed with CMR estimates of abundance (i.e., fell within the confidence bounds surrounding abundance). A subset of waterholes, with predicted turtle abundance = 0, were verified using occurrence survey data.

The size distribution of *C. rugosa* is strongly influenced by drying frequency and pig predation [3]. Populations in waterholes that dry infrequently experience low levels of recruitment because densities are close to carrying capacity (K) [5]. Populations in waterholes that dry frequently with *E. dulcis* tend to experience the highest levels of predation from pigs or harvested by humans, resulting in elevated recruitment and populations being maintained below K [3]. We used these observations to estimate K for each waterhole: (i) rarely drying waterholes with no *E. dulcis* = 5.5/ha (i.e., K = initial abundance); (ii) frequently drying waterholes with *E. dulcis* = 14.25/ha (i.e., K = 1.5 * initial abundance); (iii) frequently drying waterholes with no *E. dulcis* = 6.6/ha (i.e., K = 1.2 * initial abundance); and (iv) permanent waterholes = 3/ha. Waterholes with K < 10 animals were treated as non-viable populations (i.e., K was set to zero) in the demographic model.

Human mediated effects: pig predation and harvest rates

We hypothesized that harvest frequency (measured at 32 waterholes) and pig visitation rates (measured at 50 waterholes) were strongly influenced by the distance to the nearest outstation. We fitted models using maximum likelihood, assuming a Gaussian error distribution for logit-transformed harvest rates and a binomial error distribution for pig predation impact (measured as high or low). Model selection was performed using AIC_c. Heavy pig visitation only occurred in wetlands with high *E. dulcis* abundance (*E. dulcis*, not *C. rugosa*, is the primary target for pigs [2]), thus the relationship between pig visitation and outstation distance was modeled only for those surveyed sites with a high abundance of *E. dulcis* (n = 22).

Harvest frequency decreased with distance from the nearest outstation, and was modelled using four plausible functional forms: linear, exponential decay, logit-linear, and logit-exponential. We found the logit-exponential function to best describe the relationship between harvest and distance (logit(HARVFREQ) = 10.6*exp(-[DISTTOWN]/5.57) – 4.43). Feral pig impact (PIGROOT) increased with distance from the nearest outstation, and was modelled using two plausible

functional relationships: logit-linear or a "broken stick" logit-linear model (in which the relationship assumes different logit-linear slopes on either side of a threshold value). The modelled relationship between distance from village and probability of pig rooting and harvest was best described by the broken stick model (< 1.07 km: PIGROOT = 0, ≥ 1.07 km: logit(PIGROOT) = -0.38 + 9.28*[DISTTOWN]).

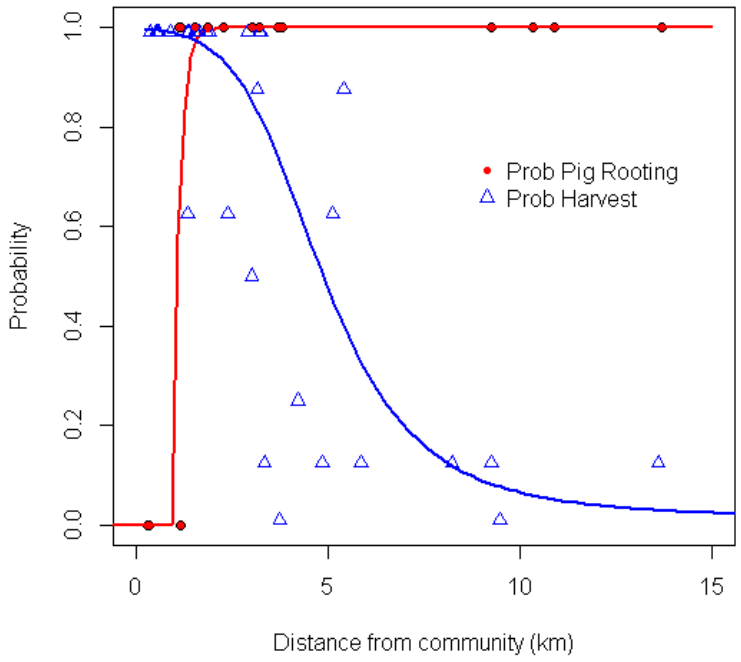

Fig. A1-1. Probability of extensive pig visitation (red) and probability of human exploitation (blue) at occupied waterholes as a function of the distance to the nearest outstation. Note that pig visitation is only displayed for waterholes with high abundance of E. dulcis.

Demographic model

We constructed spatially explicit stage- and sex-based stochastic matrix models for *C. rugosa* in RAMAS GIS v5 [18]. The model consisted of 4 female stages and 2 male stages: (i) Female S_1 = < 140mm; (ii) Female S_2 = 140-180mm; (iii) Female S_3 = > 180-220mm; (iv) Female S_4 = > 220mm; (v) Male S_5 < 140mm; (vi) Male S_6 > 140mm [4]. Previously, Fordham *et al.* [4] constructed three

baseline *C. rugosa* stage matrices describing vital rates as a function of drying, the density of *E. dulcis* and the level of pig predation. Each waterhole (with *C. rugosa* abundance > 0) was assigned one of these baseline stage matrices: (i) rarely drying waterholes = matrix 1; (ii) frequently drying waterholes with *E. dulcis* = matrix 2; (iii) frequently drying waterholes with no *E. dulcis* = matrix 1; and (iv) permanent waterholes = matrix 3 (online Appendix S3). Frequently drying waterholes with *E. dulcis* and high pig rooting occurring in < 50 % years (because they are closely located to human settlements) were assigned matrix 1.

In years of high rainfall, frequently drying waterholes do not dry [3]. This was simulated using the catastrophe function of RAMAS, whereby drying frequency was used to determine the probability of a wet year (based on Fordham *et al.* [4]) and a local multiplier was used to account for the positive effect not drying in a given year can have on abundance. Harvesting of *C. rugosa* for indigenous consumption occurs in dry years at waterholes with *E. dulcis* that are close to outstations (< 15 km away) and where pig abundance is low. We simulated harvesting using a second catastrophe function, whereby the local probability of a harvest event was defined by the probability of waterhole drying multiplied by the probability that the waterhole will be harvested (i.e., based on distance from the nearest outstation). In savanna environments, we constrained the probability of harvest to waterholes with *E. dulcis*, where pig abundance is predicted to be low. In these waterholes harvest caused a 20% decline in stage classes > 140 mm [4]. In floodplain environments, the indigenous people will catch turtles even in the presence of high densities of pigs, but the harvest rates are much lower (Fordham unpublished data). We simulated harvesting in floodplain environments up to 15 km from outstation settlements causing 10% decline in stage classes > 140 mm.

We modelled environmental variation affecting *C. rugosa* survival using CMR data [3] analysed in Program Mark with sampling variation removed [19]. We set the CV for survival in years when waterholes: (i) do not dry to 0.06 (SD = 0.057); (ii) dry with low levels of pig rooting (≤

20%) to 0.04 (SD = 0.031); and (iii) dry with high levels of pig rooting (> 20%) to 0.15 (SD = 0.089). Underwater nesting, multiple clutching and embryonic diapause buffers *C. rugosa* fecundity against environmental variation [1]. We modelled hatchling survival as density dependent. Density manipulation experiments (removal and supplementation) have shown that *C. rugosa* hatchling survival is strongly influenced by the density of turtles ≥ 140 mm [5]. Previously we modelled this relationship using a density decay function [4]. Here we use a similar approach through a function that multiplies maximum fecundities by the survival of hatchlings calculated as:

$\Phi_0 = 0.9385 * \exp(-3.88 * (N/K))$ Equation S1-1

Where N = population size, and K is the carrying capacity of animals > 140 mm.

Dispersal models

Dispersal was modelled as the proportion of individuals ≥ 140 mm [7] dispersing between each pair of defined populations during the wet season (since dispersal does not occur at other times of the year [2]). We used CMR field data, combined with expert knowledge, to model *C. rugosa* dispersal. Specifically, for any pair of populations, dispersal frequency was computed as the fraction of the total marked population at the source population that was recaptured at the target population. These observed dispersal rates were used to calibrate three different models for estimating dispersal rates between pairs of waterholes.

1. Dispersal kernel – null model: Dispersal was modeled as a function of centre-to-edge distance using a simple distance-based dispersal kernel, extrapolated from field-based estimates of average and maximum *C. rugosa* movement. Centre-to-edge was selected over the edge-to-edge method to soften the "drainage effect" by which very large populations are drained into smaller satellite populations nearby [20]. We used the dispersal-distance function,

$a * \exp(-D_{ij}^{c}/b) = 0.2 \exp(-D_{ij}^{2.4}/1.8)$ (Equation S1-2)

where D is distance from the centre of the source population to the closest edge of the target population, with a maximum recorded dispersal distance of D_{max} = 4 km (above which dispersal rate = 0). The intercept (a = 0.2) approximates the highest rate of immigration recorded from a single population. The constant b was set to 1.8 and represents mean distance between a subset of connected populations used to estimate dispersal (i.e., based on field observations). The constant c was set iteratively so that < 5 % (2.8 %) of the population moves 1.8km in a single year based on CMR data, in accord with dispersal rates observed in the field.

2. Friction-based – structural connectivity: Dispersal was modelled using a least-cost pathway method that combined a friction map (cost-of-movement raster) with the dispersal kernel described above [18], allowing dispersal to be modelled as a function of structural connectivity. We used raster algebra ("`raster`" package for R) to generate a GIS cost-of-movement ("friction") raster for the study region. Specifically, we used CMR data, observations from radiotelemetry, and expert knowledge to develop the following rules to represent cost-of-movement through a 50 m grid cell: (i) savanna habitat = 1; (ii) floodplain habitat = 0.5 (i.e., cost of moving across two floodplain cells = cost of moving across one savanna cell); (iii) freshwater wetland and stream habitat = 0.33; (iv) waterhole habitat = 0.25; and (v) salt water and dense forest habitat = 100 (i.e., cost of moving across 0.01 % of a salt water or dense forest cell = cost of moving across one savanna cell). In the dispersal kernel (Eq. S1-2), D now represents the cost-distance (cumulative cost of movement along the least-cost path) from the centre of the source population to the closest edge of the target population. In RAMAS GIS, the value 1 represents the baseline value of the cost-of-movement raster: if all grid cells in the cost-of-movement raster were set to 1, estimated dispersal rates would match the distance-based estimates derived from Eq. S1-2 [18]. Since savanna grid cell values were set to 1, and most surveyed waterholes were located in savanna environments in the cost-of-movement raster, the remaining parameters of the dispersal kernel (Eq. S1-2) were not altered for this analysis..

3. *Individual-based model – functional connectivity*: We modelled the interaction between turtle movement and habitat using a spatially explicit individual-based model (SIBM) parameterised in HexSim, which is a flexible software framework for individual-based ecological modeling and risk assessment [21]. Our mechanistic SIBM dispersal model was designed to assess dispersal rates for a single wet season (the period during which long-distance movements occur for *C. rugosa* [2]). All waterholes were initialized at carrying capacity (as described above). All turtle movements in the SIBM model were guided by an "attraction" surface (a map composed of hexagonal grid cells) that formalized four movement rules, described below. These movement rules were developed according to field observations of *C. rugosa*, and in recognition of the general dependence of this species on freshwater habitats for foraging and dispersal.

Rule 1: Dispersal movements occur during the wet season, during periods when streams are flowing and much of the floodplain is inundated [2]. We therefore assigned "attraction" values such that: (i) streams represented important movement conduits; (ii) turtle movement directions were biased downstream(high flow rates in rivers and streams during the wet season tend to carry individuals downstream [22]); and (iii) increased movement rates in floodplain environments.

Rule 2: Turtles tend to exit waterholes on the downstream side of the waterhole and move in a downslope direction when dispersing in savanna environments, presumably to locate wetlands.

Rule 3: Turtles are repelled by salt water, dense forests and the sandstone escarpment, which serve as reflective boundaries.

Rule 4: Turtles are free to leave the water catchments [6] - so the edges of the study region were modelled as absorbing boundaries. We did not consider immigration from outside the two water catchments.

The SIBM model was developed to better capture such functional elements of connectivity by including mechanisms that allowed the following biologically realistic properties to emerge: (i) turtles occupying waterholes with greater edge to area ratio are more likely to leave their home patch; (ii) turtles are more likely to successfully disperse if a site has more and larger neighbouring waterholes, and disperse further if neighbouring waterholes are closely linked by streams and rivers; and (iii) dispersing turtles are more likely to return to where they came from if neighbouring sites are mostly small and distant (*Chelodina sp.* show strong homing behaviours to favourable habitat [23]). A detailed description of the SIBM model is provided in Appendix S2.

Model Simulations

The influence of dispersal (captured using *null*, *structural connectivity*, and *functional connectivity* models) on spatial abundance patterns and local range limits was simulated using 10,000 stochastic replicates, run over a 101 year period (i.e., 2000 - 2100). Population viability was assessed using expected minimum abundance (EMA), a continuous metric reflecting risks of both declines and extinction risk [24], calculated for the period: 2010 –2100. Range movement between 2010 and 2100 was calculated annually based on the latitude of the geographic centre of the most southern sub-population [25]. Change in the number of occupied waterholes and total population abundance (of persistent model runs) over time were also investigated.

References

[1] Fordham, D., Georges, A. & Corey, B. 2006 Compensation for inundation-induced embryonic diapause in a freshwater turtle: Achieving predictability in the face of environmental stochasticity. *Funct. Ecol.* **20**, 670-677.

[2] Fordham, D., Georges, A., Corey, B. & Brook, B.W. 2006 Feral pig predation threatens the indigenous harvest and local persistence of snake-necked turtles in northern Australia. *Biol. Conserv.* **133**, 379-388.

261 [3] Fordham, D.A., Georges, A. & Brook, B.W. 2007 Demographic response of snake-necked
262 turtles correlates with indigenous harvest and feral pig predation in tropical northern Australia. *J.*
263 *Anim. Ecol.* **76**, 1231-1243.
264 [4] Fordham, D.A., Georges, A. & Brook, B.W. 2008 Indigenous harvest, exotic pig predation and
265 local persistence of a long-lived vertebrate: managing a tropical freshwater turtle for
266 sustainability and conservation. *Journal of Applied Ecology* **45**, 52-62.
267 [5] Fordham, D.A., Georges, A. & Brook, B.W. 2009 Experimental evidence for density-dependent
268 responses to mortality of snake-necked turtles. *Oecologia* **159**, 271-281.
269 [6] Alacs, E. 2008 Forensics, phylogeography and population genetics: a case study using the
270 Australasian snake-necked turtle, *Chelodina rugosa*. *PhD Thesis*. Canberra, University of
271 Canberra.
272 [7] Fordham, D. 2007 Population regulation in snake-necked turtles in northern tropical Australia:
273 modelling turtle population dynamics in support of Aboriginal harvests. *PhD Thesis*. Canberra,
274 University of Canberra.
275 [8] Kennett, R. 1992 A new trap design for catching freshwater turtles. *Wildlife Research* **19**, 443-
276 445.
277 [9] Thomson, S., Kennett, R. & Georges, A. 2000 A new species of long-necked turtle (Testudines:
278 Chelidae) from the Arnhem Land plateau, Northern Territory, Australia. *Chelonian Conservation*
279 *and Biology* **3**, 675-685.
280 [10] ESCAVI. 2003 Australian Vegetation Attribute Manual: National Vegetation Information
281 System Version 6.0. Canberra, Department of the Environment and Heritage.
282 [11] Jarvis, A., Reuter, H.I., Nelson, A. & Guevara, E. 2008 Hole-filled SRTM for the globe
283 Version 4. Available from the CGIAR-CSI SRTM 90m Database (http://srtm.csi.cgiar.org).
284 [12] Jenness, J. 2013 DEM Surface Tools. Jenness Enterprises. Available at:
285 http://www.jennessent.com/arcgis/surface_area.htm.

[13] Burnham, K.P. & Anderson, D.R. 2002 *Model Selection and Multimodel Inference, 2nd edn.* New York, Springer.

[14] McFadden, D. 1974 Conditional logit analysis of qualitative choice behavior. In *Frontiers in Econometrics* (ed. P. Zarembka), pp. 105-142, Academic Press.

[15] Nakagawa, S. & Schielzeth, H. 2013 A general and simple method for obtaining R^2 from generalized linear mixed-effects models. *Methods in Ecology and Evolution* **4**, 133-142. (doi:10.1111/j.2041-210x.2012.00261.x).

[16] Guisan, A. & Thuiller, W. 2005 Predicting species distribution: offering more than simple habitat models. *Ecology Letters* **8**, 993-1009.

[17] Swets, J. 1988 Measuring the accuracy of diagnostic systems. *Science* **240**, 1285-1293.

[18] Akcakaya, H.R. & Root, W.T. 2005 *RAMAS GIS: linking landscape data with population viability analysis (version 5.0)*. Setaukey, N.Y., Applied Biomathematics.

[19] White, G.C., Burnham, K.P. & Anderson, D.R. 2001 Advanced features of Program Mark. In *Wildlife, land, and people: priorities for the 21st century. Proceedings of the Second International Wildlife Management Congress.* (eds. R. Field, R.J. Warren, H. Okarma & P.R. Sievert), pp. 368–377. Bethesda, Maryland, USA, The Wildlife Society.

[20] Akçakaya, H.R. & Atwood, J.L. 1997 A habitat based metapopulation model of the California gnatcatcher. *Conserv. Biol.* **11**, 422-434.

[21] Schumaker, N.H. 2013 HexSim Version 2.5.7. Corvallis, Oregon, U.S. Environmental Protection Agency, Environmental Research Laboratory. Available online at http://www.hexsim.net.

[22] Rustomji, P. 2009 A statistical analysis of flood hydrology and bankfull discharge for the Daly River catchment, Northern Territory, Australia. In *Water for a Healthy Country Report*. Canberra, CSIRO.

[23] Roe, J.H. & Georges, A. 2007 Heterogeneous wetland complexes, buffer zones, and travel corridors: Landscape management for freshwater reptiles. *Biol. Conserv.* **135**, 67-76.

312 [24] McCarthy, M. & Thompson, C. 2001 Expected minimum population size as a measure of
313 threat. *Anim. Conserv.* **4**, 351-355.
314 [25] Watts, M.J., Fordham, D.A., Akçakaya, H.R., Aiello-Lammens, M.E. & Brook, B.W. 2013
315 Tracking shifting range margins using geographical centroids of metapopulations weighted by
316 population density. *Ecol. Model.* **269**, 61-69.

317

318

Appendix S2: Description of a spatial individual-based model (SIBM) model for generating pairwise dispersal rates for *Chelodina rugosa*.

We used the software HexSim [1] to construct a spatial individual-based model (SIBM) of annual dispersal rates of *Chelodina rugosa* among waterholes in two neighbouring water catchments in northern Australia (the Blythe and Liverpool rivers). Below we provide a detailed description of the SIBM model. Note that the term "HexMap" refers to a HexSim spatial data layer that stores values for each hexagonal grid cell in the landscape (i.e., a raster in which pixels are hexagons). Base spatial layers were first developed as ArcGIS ASCII Grid rasters (.ASC) as described in the Appendix S1 and were imported into HexSim using the "Generate HexMap" tool in HexSim.

GENERATE ATTRACTION SPATIAL LAYER: Prior to developing a HexSim model of annual movements, we used HexSim to generate a hexagonal raster layer (HexMap) representing the predefined attractiveness of each grid cell for *C. rugosa* movements (based on the dispersal rules described in the Appendix S1). This map was used to guide movements for all dispersal steps in the SIBM model, such that turtles moved preferentially to cells with higher values (opposite of a friction map). First, we generated a HexMap of elevation within streams and waterways (set to zero outside watercourses). This "stream elevation" layer was rescaled to vary between -15 and 15, such that the lowest elevation cells were assigned the highest values (allowing turtles to preferentially move downstream). A second elevation layer was generated, representing the elevation of each hexagon relative to the mean elevation in the surrounding region (defined as a circular region with 1 km radius). The relative elevation layer was also rescaled to vary between –15 and 15, such that the lowest relative elevations were assigned the highest values. This map layer was developed to allow turtles to display a preference to move downslope when outside of watercourses. The final attraction map was generated to follow the movement rules listed in the Methods (Appendix S1) and Appendix S1 (e.g., turtles tend to move downslope and along watercourses and other freshwater areas). We accounted for terrain in the model by assigning savanna habitats a mean value of 20 (± relative elevation layer), floodplain habitats a value of 40 (± relative elevation layer), freshwater watercourses and wetlands a value of 50 (± stream elevation layer), and delineated waterholes were assigned a value of 100 (representing

maximum attractiveness). Reflective barriers (features actively avoided by *C. rugosa*: e.g., salt water) were represented by a value of -1, which was set in all dispersal steps as a threshold for complete avoidance. Absorbing barriers (landscape boundaries) were coded in HexSim as a "barrier layer" with 100% mortality (for simplicity, we assumed turtles exiting the landscape never returned).

We describe the key model-based steps in the SBM below.

Initialize landscape

- INITIALIZE: To initialize the simulation, the landscape was initialized with *C. rugosa* individuals at carrying capacity. All turtles were initialized as adults, since long-distance dispersal in *C. rugosa* is thought to be limited to adults (≥ 140 mm) [2].

- REPLACE INDIVIDUALS: All turtles generated in the INITIALIZE step were replaced with new, identical individuals, thereby ensuring that HexSim correctly computed total displacement over the simulation (the "Displacement" report in HexSim computes total lifetime displacement only for those individuals born during the simulation time frame). First, a "reproduction" event replaced all individuals with "newborns". Subsequently, a "survival" event removed the initial individuals and a "transition" event changed all newborns into adults. The final movement event returned all individuals to "floater" status, to ensure that all turtles were potential dispersers (in HexSim, only floater individuals can engage in dispersal movements).

- SET INITIAL LOCATION: We determined the initial Patch ID (unique ID for each distinct waterhole in the landscape) for each individual. This location information, coupled with the SET FINAL LOCATION event, enabled *post hoc* compilation of a matrix describing pairwise rates of movement among waterholes (dispersal matrix) (via HexSim's "Projection Matrix" report; see below).

Initiate main dispersal sequence

- INITIAL MOVEMENT (random foraging movements): Each individual was allowed to move a specified number of hexagons (see below), with movement preferences dictated by the attraction map. Due to the high attraction of the waterholes themselves, most turtles remained within their initial wetland patch. The proportion remaining within waterholes was calibrated to match observed dispersal rates from capture-mark-recapture (CMR) data – i.e., the fraction of the total marked population at the source population that was recaptured at a specific target population. Total movement lengths (distinguished from net displacement) followed a lognormal distribution with parameters based on Fordham [2] (mean = 2 km, sd = 3 km). An absolute maximum movement distance was set at 10 km in this event. Note that this movement event was associated with no autocorrelation of movement directions, so net displacement was of much lower magnitude than the total distance moved. As with the other movement events, the maximum total movement distances (and directional autocorrelation) were calibrated such that individual net displacement distance across all movement events rarely (<0.1%) exceeded the maximum (net) dispersal distance set in the RAMAS model (4 km; see Appendix S1). Fig. S2-1 depicts movement trajectories for several representative individuals during the INITIAL MOVEMENT event.

- INITIAL DISPERSAL: To determine (1) which turtles would engage in long-distance dispersal and (2) how far they could move, we first recorded the location of each individual (whether in a patch or outside of a patch) and whether each turtle was located in a savanna or floodplain habitat type. Only those turtles located outside of a patch at the end of the INITIAL MOVEMENT step were allowed to engage in the long-distance dispersal. Maximum movement distance (total, not net displacement) was set at 10 km (in savanna habitat) or 20 km (in floodplain habitat), with moderate (10%) autocorrelation in movement directions. As with all other movement events, turtles exhibited movement preferences according to the attraction map. Turtles stopped dispersing as soon as they reached a designated patch (waterhole). Because of this stopping criterion, very few turtles located in

areas of high waterhole density moved the maximum distance in practice. However, since *C. rugosa* individuals were not expected to stop moving unless they reached suitable habitat, all turtles in this movement event continued to move until they either reached a designated waterhole or they reached the specified maximum movement distance. Fig. S2-2 depicts movement trajectories for several representative individuals during the INITIAL DISPERSAL event.

- STREAM DISPERSAL: Streams within the study catchments are generally characterized by strong currents during the wet season, and consequently water courses are expected to carry many turtles downstream and generally to enable longer-distance movements. To determine which individuals would engage in stream-assisted dispersal in the SIBM, we recorded whether or not each turtle was located in a stream course. Turtles located in stream courses were allowed to move up to a total distance of 20 km (again, the resulting net displacement distances were much smaller since movement directions were largely random). Based on the attraction map (in which lower-elevation stream hexagons are assigned higher values), turtles preferentially moved downstream. Movement directions were assigned a moderate (25%) autocorrelation, which resulted in higher net displacement distances relative to the INITIAL MOVEMENT and INTIAL DISPERSAL events. If a turtle reached a designated patch (waterhole), it stopped moving immediately. Repulsion and attraction parameters for this movement event were specified to ensure a low probability of leaving a stream. Fig. S2-3 depicts movement trajectories for several turtles during the STREAM DISPERSAL event.

- RESHUFFLE: This fourth and final movement event type ensured that turtles were distributed relatively evenly within waterholes. Due to the stopping criteria specified for the INITIAL DISPERSAL and STREAM DISPERSAL events, turtle densities tended to become concentrated at patch edges. This movement event reshuffles turtle locations within patches so that turtles are not stuck on the edges of patches (resulting in a more even distribution of densities within waterholes). Repulsion and attraction parameters for this movement event were specified to ensure turtles did not leave designated patches during this movement event. Turtles located outside of designated patches

were unaffected by the RESHUFFLE event. Fig. S2-4 depicts movement trajectories for several representative individuals during the RESHUFFLE event.

***Density dependent dispersal**:*

Dispersal is strongly influenced by food resource availability for *Chelodina* species [3, 4], thus we assumed that *C. rugosa* was more likely to disperse if conspecific densities exceeded the local carrying capacity. In addition, the density dependent dispersal steps (described below) tended to soften the "shadow" effect by which turtles stopped at the first quality site and failed to pass through to other suitable nearby patches [5]. By using a density-dependent movement step, turtles were able to move past waterholes that may otherwise "trap" large numbers of dispersing turtles, and instead move to other nearby waterholes.

- COMPUTE LOCAL DENSITIES: In this step we computed and mapped the local densities of turtles within each patch. This was accomplished by first using a "Generated HexMap" to record the total abundance of *C. rugosa* within each hexagonal raster cell. Then, we used a "quantify environment" accumulator (accumulators are individual state variables in HexSim) to record (1) the total abundance and (2) the total carrying capacity within each turtle's "explored area" (home range) − assumed to be 1 km^2 in area. By dividing the local abundance within each turtle's home range by the total carrying capacity in the same area, we were able to estimate the degree to which local densities exceeded the number of individuals that the habitat could support.

- IDENTIFY DENSITY DEPENDENT DISPERSERS: Turtles were placed into an "Exceeds K" category if local densities exceeded carrying capacity by 25%. Only turtles in this category were allowed to engage in density dependent dispersal.

- DENSITY DEPENDENT DISPERSAL: Turtles classed as density dependent dispersers were allowed to repeat the INITIAL MOVEMENT (with one modification: movement distances were set to match the INITIAL DISPERSAL event to ensure that all turtles located in crowded areas had a

chance to disperse), INITIAL DISPERSAL, and STREAM DISPERSAL. This way, DD dispersers were given a second opportunity to find a new patch.

- FINAL ATTEMPT TO FIND PATCH: Individuals remaining outside designated patches (located in the matrix) were given a final opportunity to locate a nearby waterhole: if a turtle was located within 1.5 km of a designated patch, then we assumed it could detect and move to the nearest waterhole (Roe and Georges [3] reported that a closely related *Chelodina* species engaged in routine movements among wetlands separated by 1.5 km or less). Effectively, this movement event enhanced dispersal success in regions where waterhole density was high. Fig. S2-5 depicts movement trajectories for several representative individuals during the FINAL ATTEMPT TO FIND PATCH event.

Finalize simulation

- SET FINAL LOCATION: We determined the final Patch ID (unique ID for each distinct waterhole in the landscape) for each individual.

- FINALIZE: Finally, we removed all simulated *C. rugosa* individuals using a "survival" event with 100% mortality. This step enabled HexSim to compute the total "lifetime" displacement distances for all individuals (Fig. S2-6).

Post-processing: generate dispersal matrix and analyze total annual displacement distances

Lastly, we used HexSim to compute a dispersal matrix, representing the proportion of individuals that moved from each designated patch (columns) to all other designated patches (rows). The built-in "projection matrix" report generator in HexSim accomplished this task, with the initial patch ID representing initial locations and the final patch ID after completion of the entire movement sequence representing final locations. The built-in "displacement" report in HexSim was used to compute total displacement distances for all individuals (Fig. S2-6).

References

[1] Schumaker, N.H. 2013 HexSim Version 2.5.7. (Corvallis, Oregon, U.S. Environmental Protection Agency, Environmental Research Laboratory, Available online at http://www.hexsim.net.

[2] Fordham, D. 2007 Population regulation in snake-necked turtles in northern tropical Australia: modelling turtle population dynamics in support of Aboriginal harvests. *PhD Thesis*. Canberra, University of Canberra.

[3] Roe, J.H., Brinton, A.C. & Georges, A. 2009 Temporal and spatial variation in landscape connectivity for a freshwater turtle in a temporally dynamic wetland system. *Ecological Applications* **19**, 1288-1299.

[4] Roe, J.H. & Georges, A. 2008 Terrestrial activity, movements and spatial ecology of an Australian freshwater turtle, Chelodina longicollis, in a temporally dynamic wetland system. *Austral Ecology* **33**, 1045-1056.

[5] Hein, S., Pfenning, B., Hovestadt, T. & Poethke, H.J. 2004 Patch density, movement pattern, and realised dispersal distances in a patch-matrix landscape—a simulation study. *Ecol. Model.* **174**, 411-420.

Figures

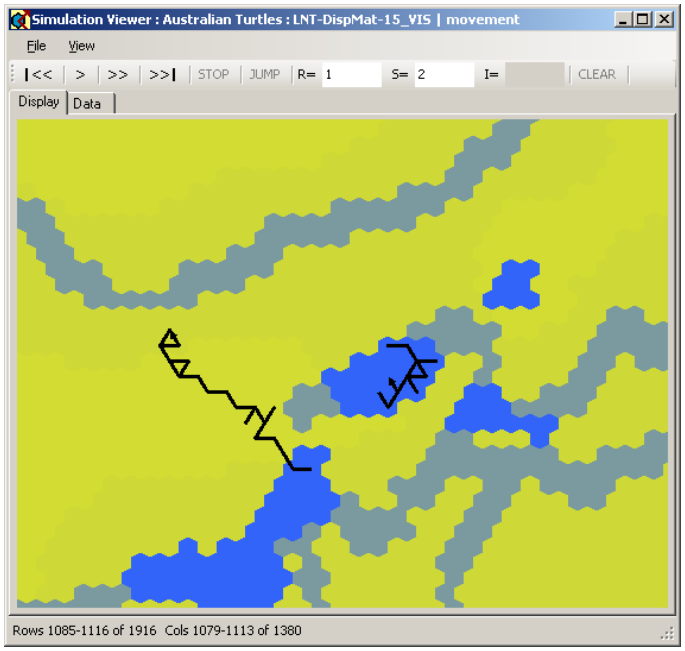

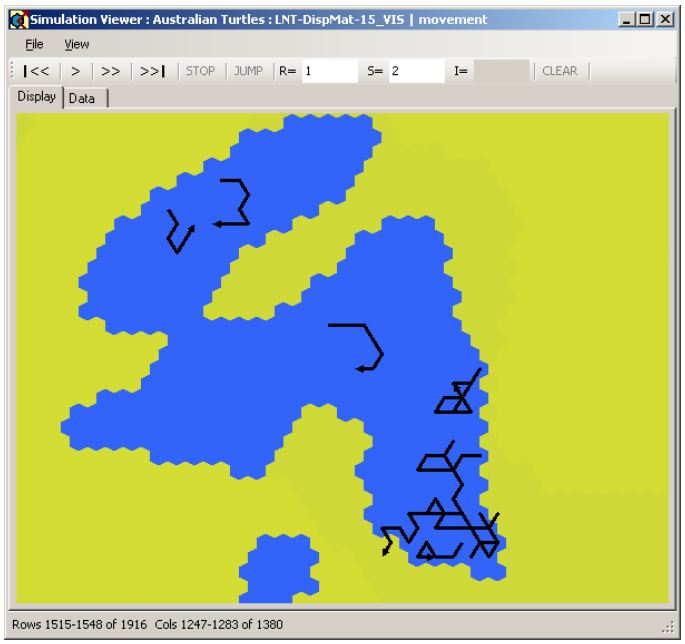

Figure S2-1. Illustrations of the INITIAL MOVEMENT event. Yellow hexagons represent savanna habitats, grey hexagons are freshwater wetlands and streams, and blue hexagons are waterholes. Movement paths are illustrated by black lines, with the initial locations and final locations (arrow head) illustrated for a representative selection of individuals. Each hexagon is 100 m across (midpoint to midpoint).

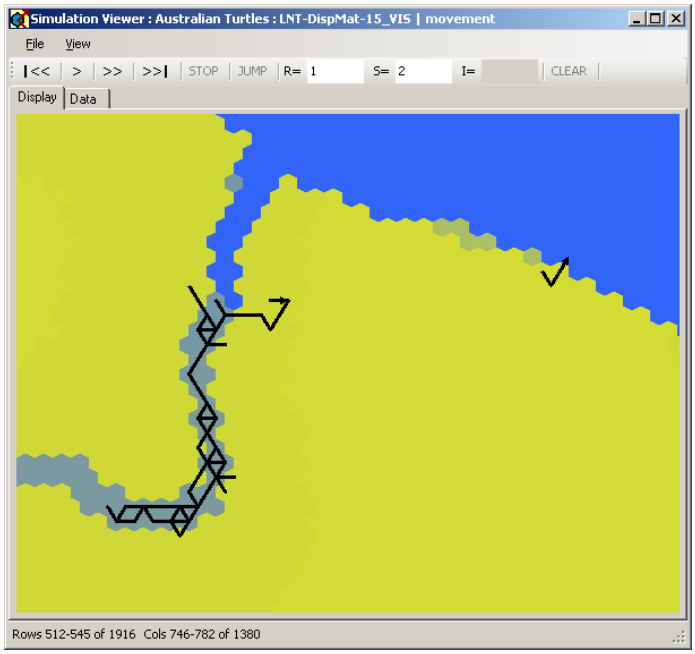

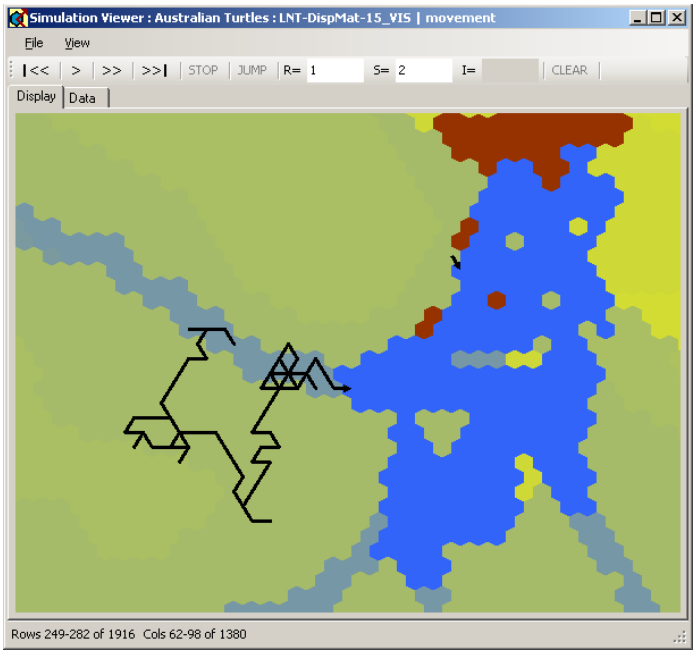

Figure S2-2. Illustrations of the INITIAL DISPERSAL event. Yellow hexagons represent savanna habitats, olive hexagons are floodplain habitats, grey hexagons are freshwater wetlands and streams, and blue hexagons are designated waterholes. Movement paths are illustrated by black lines, with the initial locations and final locations (arrow head) illustrated for a representative selection of individuals. In this movement event, turtles in floodplain habitats were capable of moving twice as far as turtles in savanna habitats.

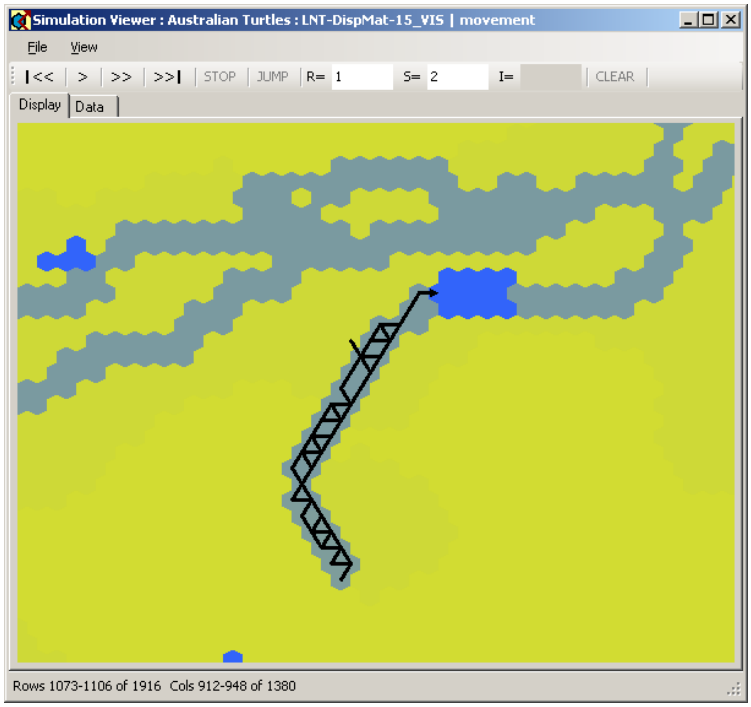

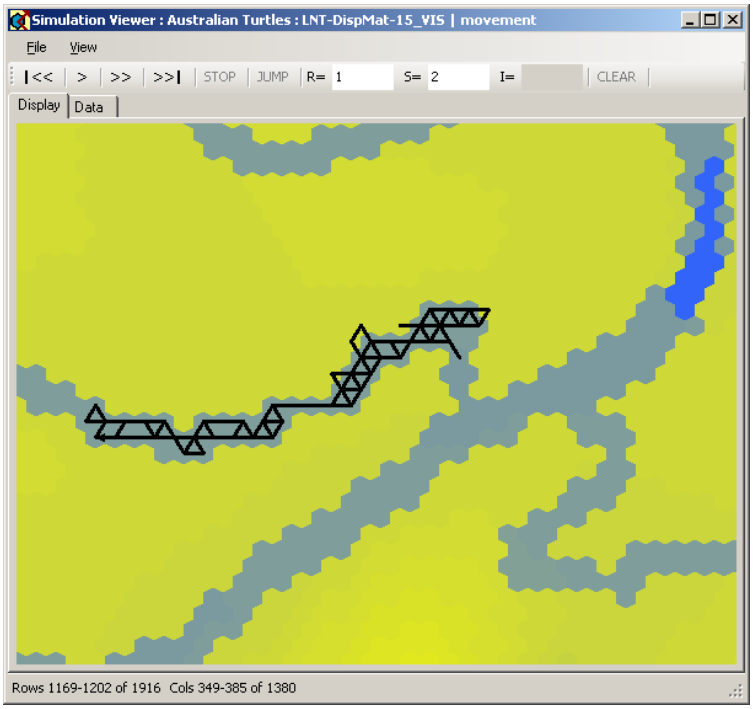

Figure S2-3. Illustrations of the STREAM DISPERSAL event. Yellow hexagons represent savanna habitats, grey hexagons are freshwater wetlands and streams, and blue hexagons are designated waterholes. Movement paths are illustrated by black lines, with the initial locations and final locations (arrow head) illustrated for representative selection of individuals.

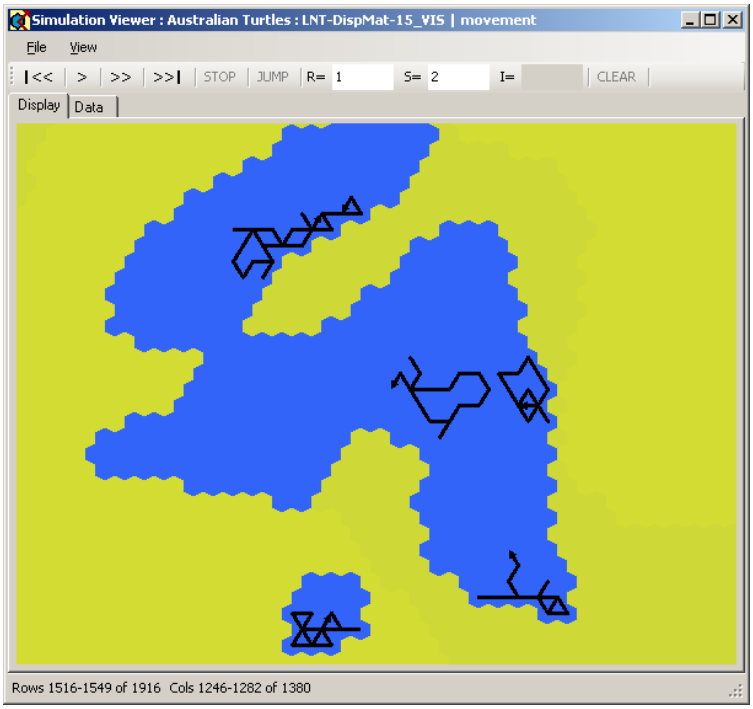

200

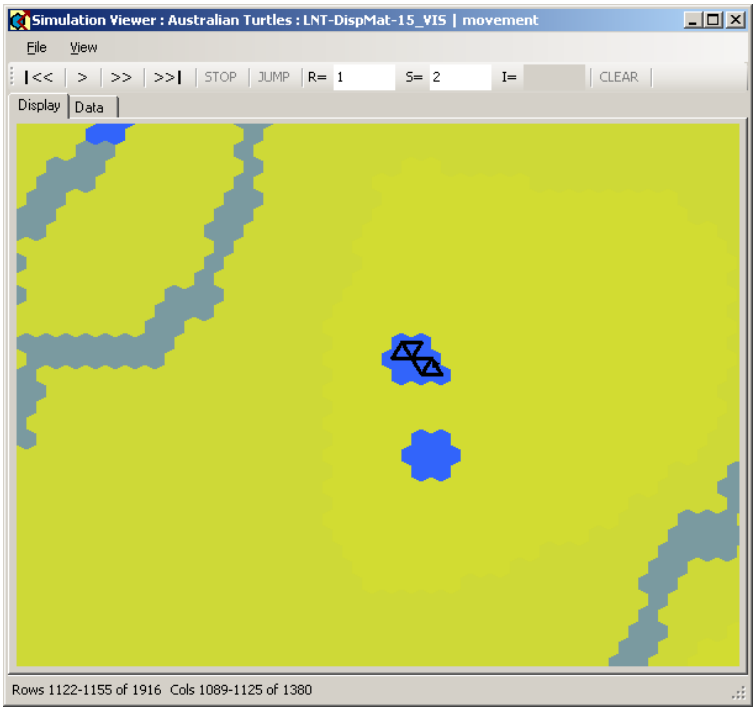

201

202 *Figure S2-4. Illustrations of the RESHUFFLE event. Yellow hexagons represent savanna habitats, grey*
203 *hexagons are freshwater wetlands and streams, and blue hexagons are designated waterholes. Movement*
204 *paths are illustrated by black lines, with the initial locations and final locations (arrow head) illustrated for*
205 *a representative selection of individuals.*

206

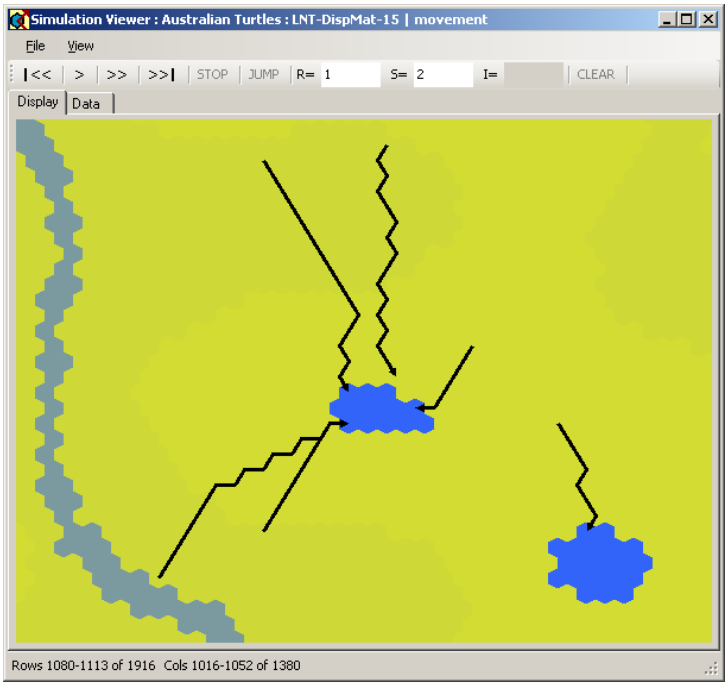

207

208 *Figure S2-5. Illustrations of the FINAL ATTEMPT TO FIND PATCH event. Yellow hexagons represent*
209 *savanna habitats, grey hexagons are freshwater wetlands and streams, and blue hexagons are designated*
210 *waterholes. Movement paths are illustrated by black lines, with the initial locations and final locations*
211 *(arrow head) illustrated for a representative selection of individuals. If one or more waterholes was*
212 *located within 1.5 km, then turtles were allowed to move to the nearest waterhole.*

213

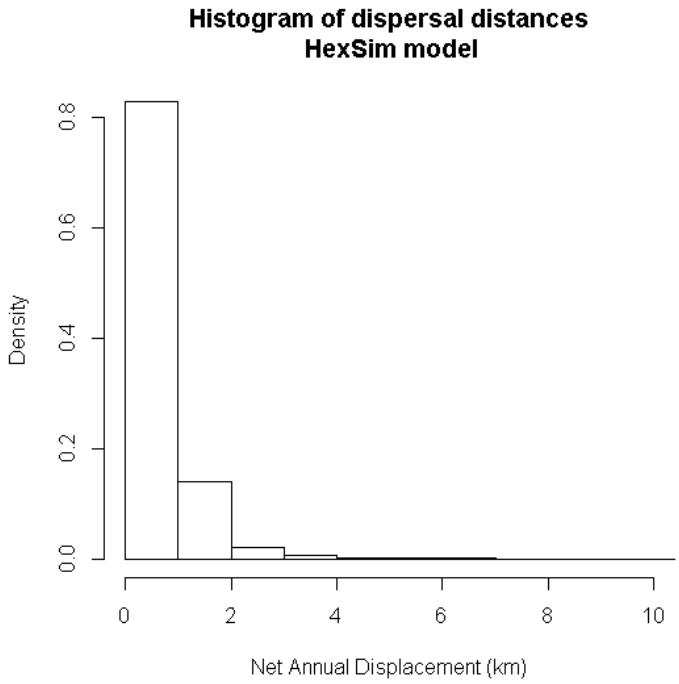

214

215 *Figure S2-6. Histogram of net movement distances for individual turtles in the SIBM model. Note that very*
216 *few turtles (<0.1%) moved more than 4 km (the maximum dispersal distance specified in the distance-based*
217 *methods), although rare outlier individuals moved as far as 7 to 10 km.*

218

Appendix S3: Pre-breeding stage matrices for *Chelodina rugosa*

		Females				Males	
		F S1 <140m	F S2 140-1	F S3 180-2	F S4 >220	M S5 <140m	M S6 >140m
Females	F S1 <140m	0.304	0.0	3.8175	5.25375	0.0	0.0
	F S2 140-1	0.53	0.418	0.0	0.0	0.0	0.0
	F S3 180-2	0.0	0.416	0.686	0.0	0.0	0.0
	F S4 >220	0.0	0.0	0.148	0.834	0.0	0.0
Males	M S5 <140m	0.0	0.0	0.23	0.316	0.304	0.0
	M S6 >140m	0.0	0.0	0.0	0.0	0.53	0.834

Matrix 1: Survival, transition and fertility rates for turtles in rarely drying waterholes, and frequently drying waterholes with no *Eleocharis dulcis* sedge. The matrix consists of: four female stages, FS1 **(**Carapace length [CL] < 140 mm), FS2 **(**CL ≥ 140 -180mm), FS3 (CL ≥ 180-200mm) and FS4 (CL ≥ 220mm); and two male stages, MS5 (CL < 140mm) and MS6 (CL ≥ 140mm).

		Females				Males	
		F S1 <140m	F S2 140-1	F S3 180-2	F S4 >220	M S5 <140m	M S6 >140m
Females	F S1 <140m	0.227	0.0	3.8175	5.25375	0.0	0.0
	F S2 140-1	0.274	0.308	0.0	0.0	0.0	0.0
	F S3 180-2	0.0	0.193	0.471	0.0	0.0	0.0
	F S4 >220	0.0	0.0	0.03	0.501	0.0	0.0
Males	M S5 <140m	0.0	0.0	0.23	0.316	0.227	0.0
	M S6 >140m	0.0	0.0	0.0	0.0	0.274	0.501

Matrix 2: Survival, transition and fertility rates for turtles in frequently drying waterholes with *Eleocharis dulcis*. Stage classes are the same as for Matrix 1 (see description above).

		Females				Males	
		F S1 <140	F S2 140-1	F S3 180-2	F S4 >220	M S5 <140	M S6 >140
Females	F S1 <140	0.321	0.0	3.8175	5.25375	0.0	0.0
	F S2 140-1	0.609	0.443	0.0	0.0	0.0	0.0
	F S3 180-2	0.0	0.487	0.731	0.0	0.0	0.0
	F S4 >220	0.0	0.0	0.199	0.93	0.0	0.0
Males	M S5 <140	0.0	0.0	3.0	4.0	0.321	0.0
	M S6 >140	0.0	0.0	0.0	0.0	0.609	0.93

Matrix 3: Survival, transition and fertility rates for turtles in permanent waterholes. Stage classes are the same as for Matrix 1 (see description above).

Online Figure S1: Final population size for refuge populations

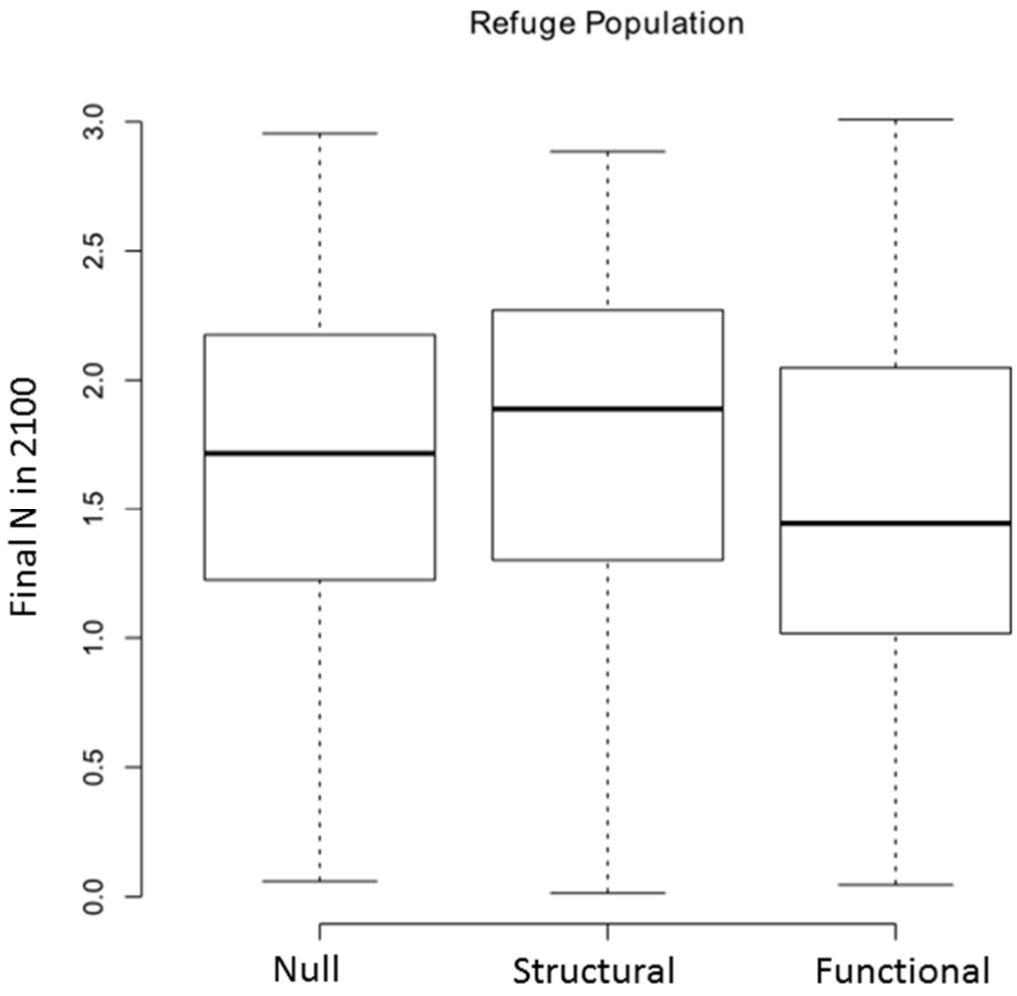

Final population size in 2100 (log10 transformed) for refuge populations derived from a stochastic metapopulation model for *Chelodina rugosa* according to three connectivity scenarios: *null*, *structural* and *functional*.

Online Figure S2: Duration of local population persistence in savannah and floodplain environments

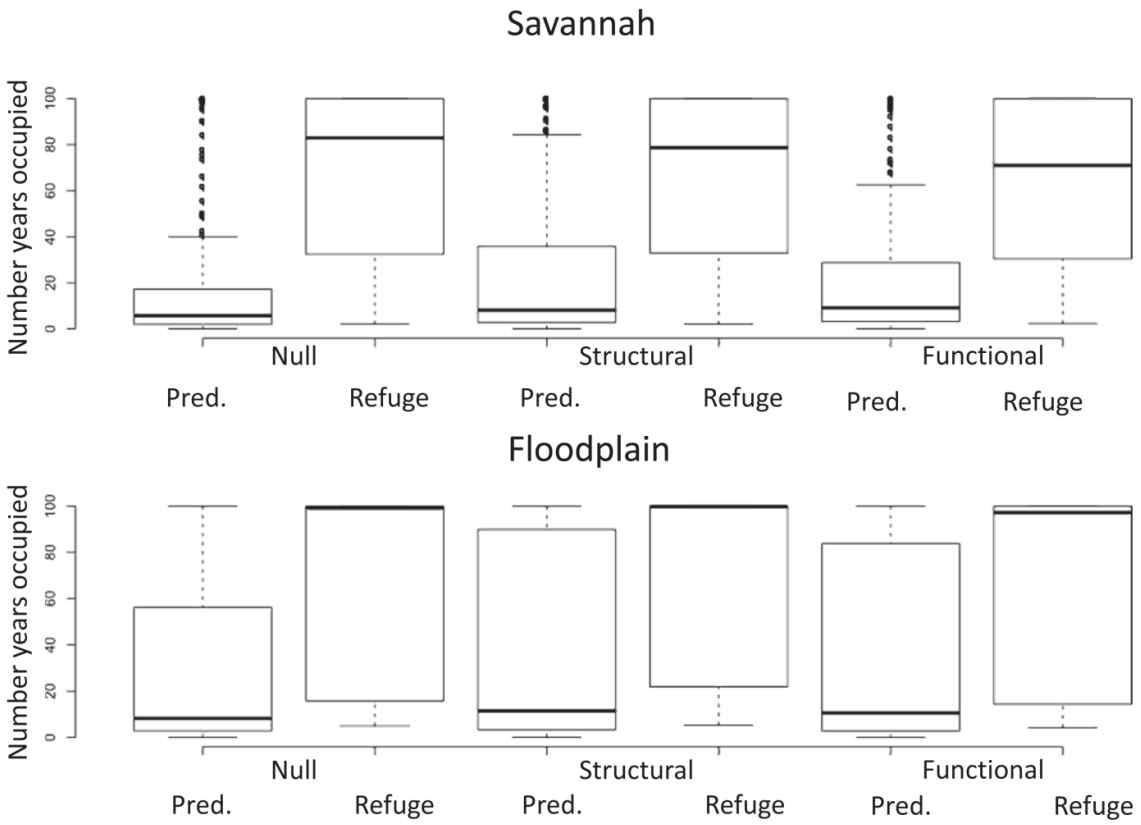

Number of years that populations persisted under high (Pred.) and low (Refuge) pig predation (and to a lesser extent harvesting by indigenous people) in savannah and floodplain habitats derived from a stochastic metapopulation model for *Chelodina rugosa* according to three connectivity scenarios: *null*, *structural* and *functional*.